BOSTER
antibody and ELISA experts

BOSTER BIOLOGICAL TECHNOLOGY
3942 B Valley Ave, Pleasanton, CA 94566
888-466-3604 | support@bosterbio.com | www.bosterbio.com

Anti-CD44 Antibody Picoband®

Catalog Number: A00052

About CD44

CD44 is also known as LHR or MC56. The protein encoded by this gene is a cell-surface glycoprotein involved in cell-cell interactions, cell adhesion and migration. It is a receptor for hyaluronic acid (HA) and can also interact with other ligands, such as osteopontin, collagens, and matrix metalloproteinases (MMPs). This protein participates in a wide variety of cellular functions including lymphocyte activation, recirculation and homing, hematopoiesis, and tumor metastasis. Transcripts for this gene undergo complex alternative splicing that results in many functionally distinct isoforms, however, the full length nature of some of these variants has not been determined. Alternative splicing is the basis for the structural and functional diversity of this protein, and may be related to tumor metastasis.

Overview

Product Name	Anti-CD44 Antibody Picoband®
Reactive Species	Human, Mouse, Rat
Description	Boster Bio Anti-CD44 Antibody Picoband® catalog # A00052. Tested in ELISA, Flow Cytometry, IF, IHC, IHC-F, ICC, WB applications. This antibody reacts with Human, Mouse, Rat. The brand Picoband indicates this is a premium antibody that guarantees superior quality, high affinity, and strong signals with minimal background in Western blot applications. Only our best-performing antibodies are designated as Picoband, ensuring unmatched performance.
Application	ELISA, Flow Cytometry, IF, IHC, IHC-F, ICC, WB
Clonality	Polyclonal
Formulation	Each vial contains 4mg Trehalose, 0.9mg NaCl, 0.2mg Na2HPO4, 0.05mg NaN3.
Storage Instructions	Store at -20˚C for one year from date of receipt. After reconstitution, at 4˚C for one month. It can also be aliquotted and stored frozen at -20˚C for six months. Avoid repeated freeze-thaw cycles.
Host	Rabbit
Uniprot ID	P16070

Technical Details

Immunogen	E. coli-derived human CD44 recombinant protein (Position: Q21-H259).
Recommended Detection Systems	Boster recommends Enhanced Chemiluminescent Kit with anti-Rabbit IgG (EK1002) for Western blot, and HRP Conjugated anti-Rabbit IgG Super Vision Assay Kit (SV0002-1) for IHC(P), IHC(F) and ICC.
Cross Reactivity	No cross-reactivity with other proteins.
Isotype	Rabbit IgG

BOSTER BIOLOGICAL TECHNOLOGY
3942 B Valley Ave, Pleasanton, CA 94566
888-466-3604 | support@bosterbio.com | www.bosterbio.com

Form	Lyophilized
Concentration	Adding 0.2 ml of distilled water will yield a concentration of 500 ug/ml.
Purification	Immunogen affinity purified.
Suggested Dilutions	Western blot, 0.1-0.5ug/ml Immunohistochemistry (Paraffin-embedded Section), 0.5-1ug/ml Immunohistochemistry (Frozen Section), 0.5-1ug/ml Immunocytochemistry, 0.5-1ug/ml Immunofluorescence, 2ug/ml Flow Cytometry (Fixed), 1-3ug/1x10^6 cells ELISA, 0.1-0.5ug/ml

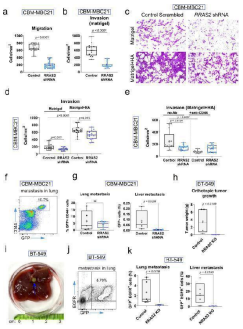

R-RAS2 is downstream of CD44 promoting migratory, invasive and metastatic behavior of breast can whiskers plot showing all experimental points of a migration assay in Boyden chambers separated by membrane. Cells were incubated overnight (~16 h). Each point represents the mean of cells per surf membrane counted. A number of 18 areas of the membrane were counted per experimental conditio significance was assessed by carrying out a Mann-Whitney test. b , Box and whiskers plot showing al a migration assay in Boyden chambers separated by a 8 um-diameter pore membrane and layered o with 100 uL of Matrigel. Cells were incubated overnight (~16 h). Each point represents the mean of c (mm 2) of membrane counted. A number of 18 areas of the membrane were counted per experimen significance was assessed by carrying out a Mann-Whitney test. c , Light field microscopy of the botto membrane with 8-um diameter pores separating an upper Boyden chamber in which CBM-MBC21 co were seeded in serum-free medium and a lower chamber containing medium with 20% feta bovine s upper chamber had a layer or either Matrigel or Matrigel + hyaluronic acid directly on top of the me allowed to migrate for 8 h from the top to the bottom chambers and through the Matrigel or Matrigel bottom part of the membrane was stained with crystal violet to count the number of migrated cells. plot showing all experimental points of the experiment illustrated in Fig. c. Each point represents the surface unit (mm 2) of membrane counted. A number of 14 areas of the membrane were counted pe condition. Statistical significance was assessed using unpaired t-tests. e , An invasion assay as this o carried out in Boyden chambers coated in the upper chamber with a layer of Matrigel + hyaluronic a knockdown CBM-MBC21 cells were incubated or not (no Ab) with 5 ug/mL of blocking anti-CD44 antib chamber for 8 h. Box and whiskers plot showing all experimental points that represent the mean of c (mm 2) of membrane counted. A number of 13–14 areas of the membrane were counted per experi Statistical significance was assessed using a one-way ANOVA Tukey's multiple comparison test. f , Th of control and knockdown CBM-MBC21 cells 25 days after orthotopic inoculation in the left inguinal m female C57BL/6 mice was assessed by flow cytometry of the lungs and liver. The pseudocolor plot sh of metastatic breast cancer cells in the lungs according to the expression of GFP and CD44. g , Box a showing all experimental points calculated as illustrated in Fig. f and Suppl Fig. f referring to BC cell i liver, respectively. Each point represents a single mouse. Statistical significance was assessed by ca Whitney tests. h , Box and whiskers plot showing all experimental points indicating primary tumor we with BT-549 human BC cells at the day of sacrifice (day 39). Statistical significance was assessed by Whitney test. i , Photograph of the entire liver taken from a mouse inoculated with wild type BT-549, blue arrow points at the presence of a green fluorescent BC tumor nodule. j , The metastatic capacity knockdown BT-549 cells 39 days after orthotopic inoculation in the left inguinal mammary gland of fe gammac −/− mice was assessed by flow cytometry of the lungs and liver. The two-color plot shows t metastatic breast cancer cells in the lungs according to the expression of GFP and human EGFR. k , B showing all experimental points calculated as illustrated in Fig. j referring to BC cell infiltration of lun four liver lobules per animal were processed for flow cytometry analysis. Each point represents a sing significance was assessed by carrying out Mann-Whitney tests Index in PubMed under a CC BY licens

Western blot analysis of CD44 using anti-CD44 antibody (A00052). Electrophoresis was performed on at 70V (Stacking gel) / 90V (Resolving gel) for 2-3 hours. The sample well of each lane was loaded wi under reducing conditions. Lane 1: human U251 whole cell lysates, Lane 2: rat lung tissue lysates, La intestine tissue lysates, Lane 4: mouse lung tissue tissue lysates. After electrophoresis, proteins were nitrocellulose membrane at 150 mA for 50-90 minutes. Blocked the membrane with 5% non-fat milk/

BOSTER BIOLOGICAL TECHNOLOGY
3942 B Valley Ave, Pleasanton, CA 94566
888-466-3604 | support@bosterbio.com | www.bosterbio.com

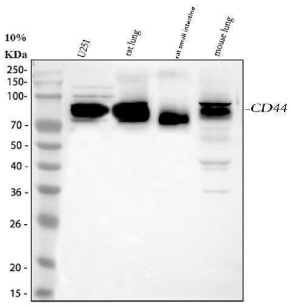

The membrane was incubated with rabbit anti-CD44 antigen affinity purified polyclonal antibody (Cat ug/mL overnight at 4°C, then washed with TBS-0.1%Tween 3 times with 5 minutes each and probed w IgG-HRP secondary antibody at a dilution of 1:5000 for 1.5 hour at RT. The signal is developed using Chemiluminescent detection (ECL) kit (Catalog # EK1002) with Tanon 5200 system. A specific band w at approximately 82 kDa. The expected band size for CD44 is at 82 kDa.

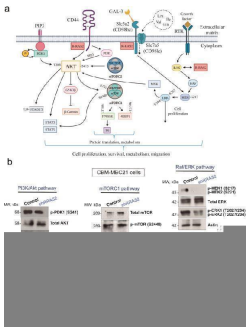

R-RAS2 controls PI3K/Akt, ERK/MAPK and mTORC1 pathway activation in murine RRAS2-overexpressi a , Cartoon illustrating RAS/ERK/MAPK, PI3K/Akt and mTORC1 pathway activation by Receptor Tyrosin EphaA2, EGFR or HER2, and by amino acid transporters like the CD98hc/CD98lc(LAT1) complex, and of some relevant phosphorylated residues are indicated, as well as the putative position of R-RAS2 do CD44 and CD98. b , Western blot analysis of signaling pathway activity based on the phosphorylation elements indicated. Post-nuclear cell lysates of wild type CBM-MBC21 cells and a shRNA-generated R that cell line were analyzed in the blots. c , Summary of the results generated by Western blot. The in RAS2 depletion is indicated by the number of arrows pointing downwards Index in PubMed under a C 40221767

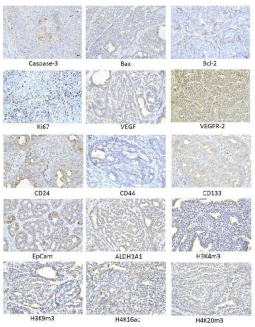

Representative images of the expression of caspase-3, Bax, Bcl-2, Ki67, VEGFA, VEGFR-2, MDA, CD24 EpCam, H3K4m3, H3K9m3, H4K20m3, H4K16ac in rat carcinoma tissue of mammary gland. For detec caspase-3 antibody (Bioss, Woburn, USA), polyclonal Bax and Bcl-2 antibodies (Santa Cruz Biotechno USA), monoclonal Ki67 antibody (Dako, Glostrup, Denmark), monoclonal VEGFA and VEGFR-2 antibod Biotechnology, Paso Robles, CA, USA), polyclonal CD24 antibody (GeneTex, Irvine, CA, USA), polyclon (Boster, Pleasanton, CA, USA), polyclonal ALDH1A1 antibody (ThermoFisher, Rockford, IL, USA), polyc H3K4m, H3K9m3, and H4K20m3 antibodies (Abcam, Cambridge, MA, USA), and monoclonal H4K16ac Cambridge, MA, USA) were applied; final magnification: ×400.Index in PubMed under a CC BY license

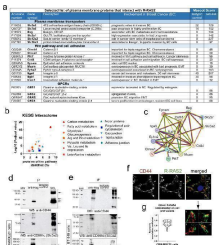

R-RAS2 interacts with plasma membrane receptors known to be important for breast cancer. a , Sele membrane proteins that interact with R-RAS2 in a murine breast cancer tumor isolated from a Rosa2 Cre female mouse. Full data can be found in Extended Data Table . The known involvement of these breast cancer is briefly summarized, and the Mascot Score for the specific affinity column with anti-h hemagglutinin-tagged R-RAS2) and a control isotypic immunoglobulin column is also shown. Protein f association with cancer data have been retrieved from The Human Protein Atlas: . b , Biological proce found to be significantly altered after KEGG analysis of the R-RAS2 plasma membrane interactome of The x-axis shows the percentage or proteins in the pathway found associated to R-RAS2 and the y-ax adjusted value. Full data is provided in Extended Data Table . c , STRING network of physical and fun among the indicated proteins from Fig. a. Pink lines indicate experimentally-determined interactions; interactions found in curated databases; green lines indicate interactions found by textmining and bl expression. d , Co-immunoprecipitation of CD44, Epha2 and Slc3a2 (CD98hc) with R-RRAS2 (IP anti-H detergent lysates of the CBM-MBC21 mouse cell line. The membranes were re-probed with anti-Hag a of R-RAS2, and the arrows indicate the positions of the co-immunoprecipitated proteins and those in (WCL). The molecular weight markers are shown on the left. e , Co-immunoprecipitation of CD44, Eph (CD98hc) with R-RRAS2 in detergent lysates of the human breast cancer cell line BT-549 transfected RAS2 construct. Legend as in panel d . f , Mid-plane confocal microscopy sections of CBM-MBC21 cells R-RAS2 (anti-Hag) and anti-CD44 antibodies to show their co-localization at the plasma membrane. T is stained with DAPI (blue). Details of 4 areas of the plasma membranes are shown to the right to sho R-RAS2 with CD44 in cell protrusions. g , Co-localization of R-RAS2 and CD44 was measured by analy cell protusions as in the inset of Fig. f and calculating the Pearson's correlation coefficient. The violin points, the median (= 0.70) and the 75% and 25% percentiles. h , Mid-plane confocal microscopy sec cells fixed and stained with R-RAS2 (anti-Hag) and anti-CD98hc antibodies to show their co-localizatio

BOSTER BIOLOGICAL TECHNOLOGY
3942 B Valley Ave, Pleasanton, CA 94566
888-466-3604 | support@bosterbio.com | www.bosterbio.com

membrane. The nucleus of the cells is stained with DAPI (blue). Details of 4 areas of the plasma mem
the right to show the co-localization of R-RAS2 with CD98hc at the external (apical) plasma membran
i , Co-localization of R-RAS2 and CD98hc was measured by analysis of all pixels in 25 membrane regi
Fig. h and calculating the Pearson's correlation coefficient. The violin plot shows all data points, the n
75% and 25% percentiles Index in PubMed under a CC BY license. PMID: 40221767

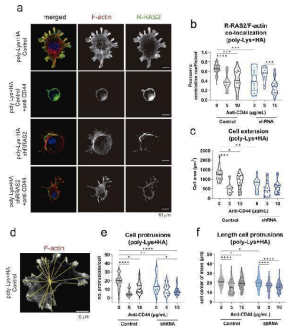

R-RAS2 co-localizes with CD44 in F-actin-rich cell protrusions of breast cancer cells. a , Confocal micr
plane of contact with the coverslips of CBM-MBC21 control and knockdown cells plated on coverslips
lysine alone or with poly-L-lysine plus hyaluronic acid (HA). Cells were plated in the presence or abse
CD44 antibody. After incubation, cells were fixed and stained with R-RAS2 (anti-Hag) and phalloidin t
localization at sites rich in F-actin. The nucleus of the cells is stained with DAPI (blue). b , Co-localizat
actin at cell protrusions was measured by analysis of all pixels in 17–33 cell protrusions and calculati
correlation coefficient. The violin plot shows all data points, the median and the 75% and 25% percer
condition. Statistical significance was assessed using a one-way ANOVA Tukey's multiple comparison

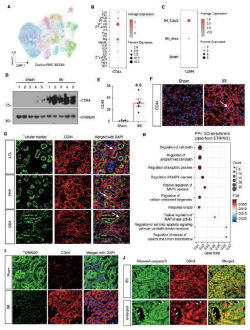

CD44 is upregulated in TECs and associated with mitochondrial dysfunction and apoptosis. A UMAP sl
kidneys of sham and IRI at 6 h and day 2. PT proximal tubule, PT-Inj injured PT, PT-R repairing PT, FR-
cell, PT-AcInj acute injury PT, DTL descending limb of loop of Henle (LoH), ATL thin ascending limb of
ascending limb of LoH, DCT distal convoluted tubule, CNT connecting tubule, PC principal cell of colle
intercalated cell of collecting duct, ICB type B intercalated cell of collecting duct, Pod podocyte, EC en
fibroblast, Myofib myofibroblast, Ma macrophage (Mphi), B/T immune cell, Uro urothelium. Data from
Graphic presentation of single-cell sequencing analysis shows the expression of CD44 in different cel
presentation of single-cell sequencing analysis shows the expression of CD44 at different time point.
Representative western blot of CD44 (D) and graphical presentations (E) of protein expressional le

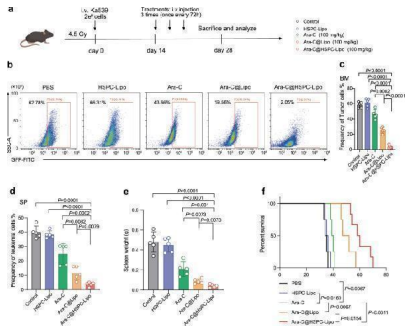

The anti-leukemic effect of Ara-C@HSPC-Lipo in Ka539 leukemia model. a Schematic illustration of ar
design. Cell membranes were derived from primary isolated HSPCs. Each received approximately 20
ug of cell membrane. b Representative flow cytometry plots of leukemia cells (GFP positive cells) in b
mice were euthanized at day 28 to collect bone marrow cells for analysis. c Quantitative analysis of l
marrow. Data were presented as mean ± s.d. (n = 5 mice). d Quantitative analysis of leukemia cells
presented as mean ± s.d. (n = 5 mice). e Weight of Spleen. Data were presented as mean ± s.d. (n
curves of the leukemic mice received different treatments. The statistics and P -values were calculate
(Mantel-Cox) test. (n = 6 mice for control, HSPC-Lipo and Ara-C group, and n = 8 mice for Ara-C@Lip
Ara-C@HSPC-Lipo group). Statistical significance of P values was calculated via a two-tailed, unpaired
were indicated as * P

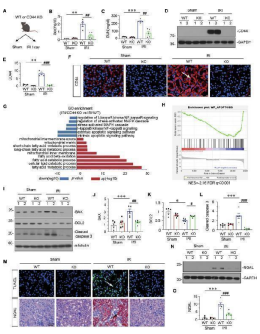

Gene ablation of CD44 attenuates renal tubular cell apoptosis and kidney injury upon IRI. A Experime
mice and CD44 conventional knockout mice were subjected to IRI or sham, respectively, and euthani
levels in four groups, as indicated. Scr was expressed as milligrams per deciliter. ** P

CD44 knockout ameliorates mitochondrial dysfunction and FAO deficiency in IRI mice. A GSEA shows
of mitochondrial function and FAO was enriched in CD44 knockout mice versus wild-type mice upon I
enrichment score; FDR q -value<0.25. B Graphic presentation shows the relative levels of renal expre
mRNA in different groups as indicated. *** P

BOSTER BIOLOGICAL TECHNOLOGY
3942 B Valley Ave, Pleasanton, CA 94566
888-466-3604 | support@bosterbio.com | www.bosterbio.com

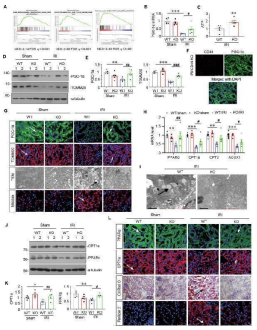

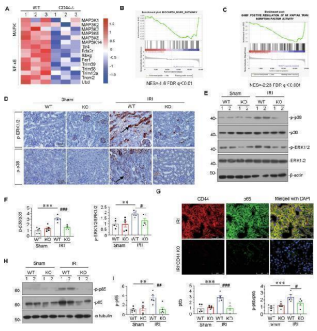

CD44 promotes AKI progression through inducing MAPK and NF-kappaB p65 signaling. A Representat
expression of RNA sequencing analysis shows that CD44 is involved with MAPK and NF-kappaB signal
GSEA shows that negative regulation of MAPK and NF-kappaB pathway was enriched in CD44 knocko
type mice upon IRI. NES, normalized enrichment score; FDR q -value<0.25. D Representative microgr
expression of p-ERK1/2 and p-p38 in different groups, as indicated. Paraffin sections were stained wit
ERK1/2 and p-p38. Arrows indicate positive staining. Scale bar, 50 um. E and F Representative weste
graphical presentations of p-p38/p38 and p-ERK1/2/ERK1/2 protein levels are shown. ** P

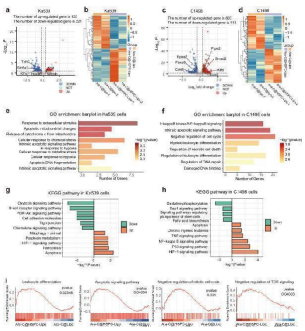

Transcriptome analysis reveals mechanisms of Ara-C@HSPC-Lipo treatment. a Volcano plot of differe
Ka539 cells. b Heat map of clustering analysis of differential gene in Ka539 cells. c Volcano plot of dif
expression in C1498 cells. d Heat map of clustering analysis of differential gene in C1498 cells. e GO
analysis in Ka539 cells. f GO pathway enrichment analysis in C1498 cells. g KEGG enrichment analysi
KEGG enrichment analysis in C1498 cells. i Enrichment analysis of GSEA gene set in C1498 cells. The
P values were derived from a two-sided statistical test (a, c) or one-sided statistical test (e – i) and
multiple comparisons. Index in PubMed under a CC BY license. PMID: 38971796

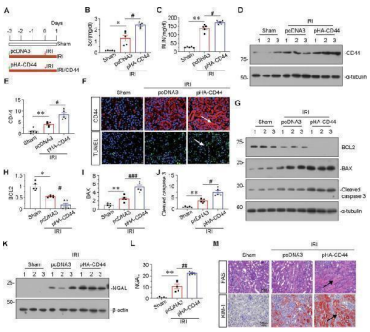

Ectopic CD44 aggravates tubular cell apoptosis and kidney injury in IRI mice. A Experimental design:
the injection of pcDNA3 plasmid or p-HA-CD44 overexpression plasmid. Mice were subjected to IRI su
respectively, as shown in the red arrow. Mice are euthanized 24 h after surgery. B Scr levels in three
Scr was expressed as milligrams per deciliter. * P

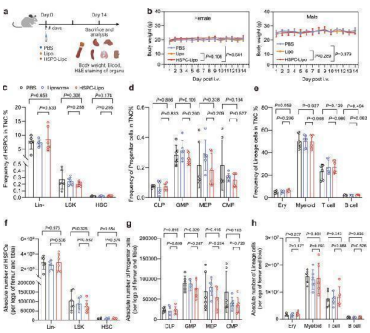

Safety evaluation and analysis of HSPC-Lipo. a Schematic illustration of animal experiment design. b
different treatment groups. Data represent the mean ± s.d. (n = 6 mice). c Quantitative analysis of H
progenitor cells in total mononuclear cells. d Quantitative analysis of progenitor cells in total mononu
Quantitative analysis of lineage cells in total mononuclear cells. f Quantitative analysis of absolute nu
stem progenitor cells per legs of tibia and femur. g Quantitative analysis of absolute number of proge
tibia and femur. h Quantitative analysis of absolute number of lineage cells per legs of tibia and femu
The data represent the mean ± s.d (c – h). Statistical significance of P values was calculated via a tw
Student's t test and were indicated as * P

BOSTER BIOLOGICAL TECHNOLOGY
3942 B Valley Ave, Pleasanton, CA 94566
888-466-3604 | support@bosterbio.com | www.bosterbio.com

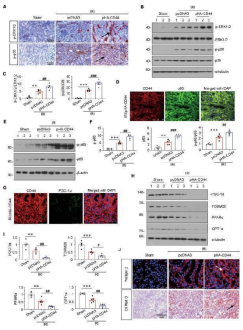

Ectopic expression of CD44 impairs mitochondrial function and FAO through activating MAPK and NF-
A Representative micrographs show the expression of p-ERK1/2 and p-p38 in different groups, as indi
were stained with antibodies against p-ERK1/2 and p-p38. Arrows indicate positive staining. Scale bar
Representative western blot (B) and graphical presentations of p-ERK1/2/ERK1/2 and p-p38/p38 pro
** P

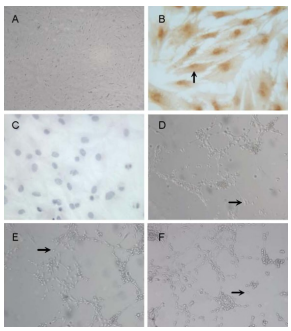

Morphology of neuron-like cells derived from rat bone marrow mesenchymal stem cells. (A, D–F) Inve
microscope, × 100; (B, C) immunocytochemical staining, × 400. (A) Passage 3 bone marrow mesench
Bone marrow mesenchymal stem cells were positive for CD44 (arrow, cytoplasmic staining was brow
marrow mesenchymal stem cells were negative for CD34. (D) Neuron-like cells (arrow) derived from
mesenchymal stem cell induced by basic fibroblast growth factor 8 and Xiangdan injection for 3 hour
(arrow) derived from rat bone marrow mesenchymal stem cells induced by basic fibroblast growth fa
acid and glial cell line-derived neurotrophic factor for 6 days. (F) Neuron-like cells (arrow) derived fro
mesenchymal stem cells induced by basic fibroblast growth factor, sonic hedgehog and fibroblast gro
days.Index in PubMed under a CC BY license. PMID: 25206684

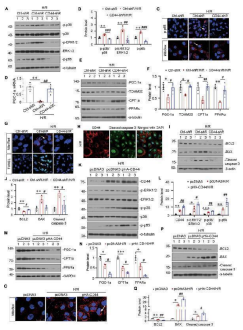

CD44 aggravates mitochondrial and FAO dysfunction and drives cell apoptosis through MAPK and NF-
in vitro. A and B HKC-8 was transfected with Ctrl-shR or CD44-shR and then were incubated in basal
O 2 environment for 24 h and then were reoxygenated in normal O 2 for 6 h. Representative western
presentations of p-p38/p38, p-ERK1/2/ERK1/2, and p-p65 protein expression levels are shown. ** P

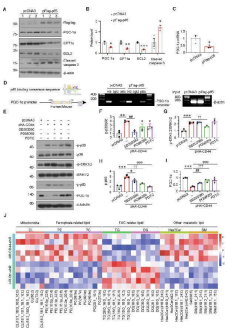

CD44 induces tubular cell injury through MAPK-NF-kappaB p65-silenced PGC-1alpha signaling. A and
transfected with pcDNA3 or p-Flag-p65 overexpression plasmid for 24 h. Representative western blot
presentations of PGC-1alpha, CPT1a, BCL2, and cleaved caspase 3 protein expression levels are show

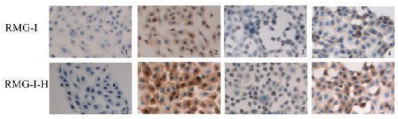

The expression of CD44 in RMG-I and RMG-I-H cells detected by immunocytochemistry (×400) . Pane
controls; panels 2 and 6 are Lewis y antibody-untreated cells; panels 3 and 7 are Lewis y antibody-tre
and 8 are cells treated by irrelevant isotype-matched control. The expression of CD44 was detected b
RMG-I and RMG-I-H cells, and brown color degree by DAB staining indicated the expression level of C
from the figure that the expression of CD44 in the RMG-I-H cells was stronger than that in RMG-I cells
after Lewis y antibody blocking. Index in PubMed under a CC BY license. PMID: 21294926

CD44 promotes tubular cell injury and AKI partially through ferroptosis. A HKC-8 was transfected with
plasmid and then treated with 5 uM erastin for 24 h. Representative micrographs show the Fe 2+ con
staining in different groups, as indicated. Scale bar, 25 um. B and C Quantitative results of QPCR sho

BOSTER BIOLOGICAL TECHNOLOGY
3942 B Valley Ave, Pleasanton, CA 94566
888-466-3604 | support@bosterbio.com | www.bosterbio.com

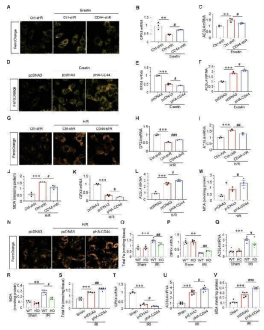

and (C) ACSL4 mRNA levels among different groups. ** P

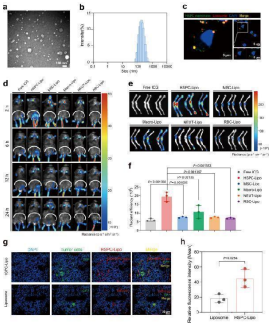

Characterization and bone marrow targeting of HSPC-Lipo. a The representative TEM images of HSPC
nm. b The average particle size distribution of HSPC-Lipo. Measured by Dynamic Light Scattering. c T
immunofluorescence confocal images of co-localization of HSPC cell membrane and liposome. HSPC c
labeled with DiO (green), liposome was labeled with DiD (red). Scale bar, 5 um. d Representative fluo
ICG fluorescent labeled different leukocyte membrane-coated liposomes in leukemic mice (Ka539 mo
subjected to in vivo imaging detection at different time intervals (2, 6, 12, 24 hours) after tail vein inj
liposomes. Each received approximately 20 ug of liposomes and 10 ug of cell membrane (indicated b
protein weight). n = 3 mice. e Representative fluorescence images of different leukocyte membrane-
the tibia and femur of mice. Mice were sacrificed at 24 h after tail vein injection of different liposome
were taken for in vivo imaging detection. n = 3 mice. f Quantitative analysis of different liposomes in
were presented as mean ± s.d. (n = 3 mice). g Representative immunofluorescence images of HSPC
Scale bar, 20 um. h Quantitative analysis of immunofluorescence results. The data were presented as
mice). Statistical significance of P values was calculated via a two-tailed, unpaired Student's t test an

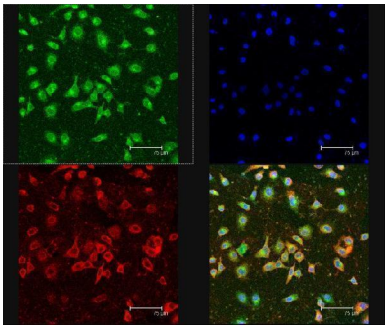

Co-location of CD44 and Lewis y antigen on RMG-I-H cells observed under confocal laser scanning mi
fluoscence on the upper left panel indicates CD44 expression; green fluoscence on the upper right pa
antigen expression; blue fluoscence on the upper right panel indicates cell nuclear location; the lowe
merged image of the other three panels. Lewis y antigen CD44 mainly expressed in the cell membran
confocal laser scanning microscope, and it were seen as yellow fluorescence after the two overlap, su
antigen and CD44 co-localizated in the cell membrane. Index in PubMed under a CC BY license. PMID

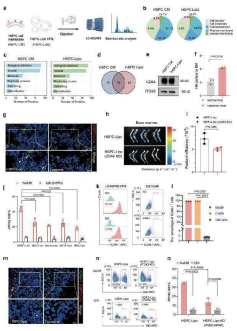

HSPC-Lipo exhibits higher affinity to leukemic cells. a Schematic illustration of Liquid chromatography
spectrometry (LC-MS/MS) sequencing design of HSPC cell membrane and HSPC-Lipo. The HSPCs cells
C57BL/6 mice. b Protein type analysis diagram. c Protein pathway enrichment analysis. d Proteins tha
membrane and HSPC-Lipo. e Western blot analysis of CD44 and ITGB2. f Determination of hyaluronic
bone marrow. Data were presented as mean ± s.d. (n = 3 mice). g Representative immunofluoresce
localization of hyaluronic acid and HSPC-Lipo. Scale bar, 10 um. h Representative fluorescence image
HSPC-Lipo at 24 hours after tail vein injection (cell membrane derived from progenitor cell line 32D c
Quantitative analysis of fluorescence images of CD44 knockdown HSPC-Lipo. Data were presented as
mice). j Flow cytometry detection of leukemic cell targeting ability of different leukocyte membrane-c
Leukemia cells were harvested for detection at 0.5 hours after incubation with different liposomes. n
replicates. k Representative flow cytometry histograms and cytometry plots of ICAM-1 expression on
and mouse progenitor cell line (32D). l Quantitative analysis of ICAM-1 expression. n = 3 experimenta
Representative immunofluorescence images of co-localization of ICAM-1 and HSPC-Lipo. Scale bar, 10
flow cytometry plots of the leukemic cells targeting ability of ITGB2 knockdown HSPC-Lipo (cell memb
mouse progenitor cell line 32D). Leukemic cells were harvested for detection 0.5 hours after incubati
liposomes. o Quantitative analysis of the leukemic cells targeting ability of ITGB2 knockdown HSPC-Li
replicates. The data were presented as mean ± s.d. Statistical significance of P values was calculated
unpaired Student's t test and were indicated as * P

BOSTER BIOLOGICAL TECHNOLOGY
3942 B Valley Ave, Pleasanton, CA 94566
888-466-3604 | support@bosterbio.com | www.bosterbio.com

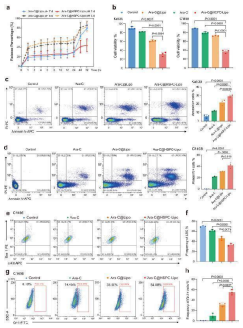

Drug loading and in vitro toxicity against leukemia cells. a Drug release kinetics of HSPC-Lipo. Data w ± s.d. (n = 3 experimental replicates). b Cell viability assay of leukemic cells after different treatmer Data were presented as mean ± s.d. (n = 3 experimental replicates). c Representative flow cytomet quantitative analysis of Annexin V positive cells after 48 hours of different treatment in Ka539 leuker presented as mean ± s.d. (n = 3 experimental replicates). d Representative flow cytometry plots an of Annexin V positive cells after 48 hours of different treatment by in C1498 leukemia cells. The leuke harvested at 48 h after different treatments and displays the same number of cells in each flow cyto presented as mean ± s.d. (n = 3 experimental replicates). e Representative flow cytometry plots of (Sca-1+c-Kit +) after 48 hours of different treatment in C1498 cells. f Quantitative analysis of LSC in presented as mean ± s.d. (n = 3 experimental replicates). g Representative flow cytometry plots of hours of different treatment in C1498 cells. h Quantitative analysis of mature cells in C1498 cells. n = replicates. The data were presented as mean ± s.d. Statistical significance of P values was calculated unpaired Student’s t test and were indicated as * P

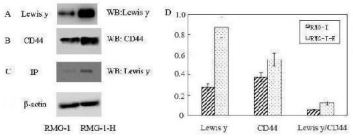

The expression of CD44 and Lewis y antigen in RMG-I and RMG-I-H cells . Panel A shows the expressio RMG-I-H cells was higher than that in RMG-I; panel B shows the expression of CD44 in RMG-I-H cells w RMG-I; panel C shows that Lewis y antigen, which in RMG-I-H cells was higher than that in RMG-I, was RMG-I and RMG-I-H cells after CD44 immunoprecipitation; panel D Quantitative data were expressed target genes to beta-actin. (P < 0.01) Index in PubMed under a CC BY license. PMID: 21294926

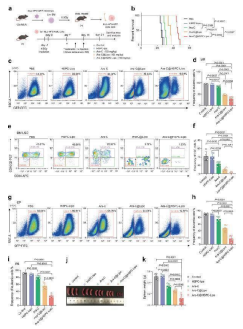

The anti-leukemic effect of Ara-C@HSPC-Lipo in MLL-AF9 leukemia model. a Schematic illustration of design. Cell membranes were derived from primary isolated HSPCs. Each received approximately 20 ug of cell membrane. b Survival curves of the leukemic mice received different treatments. The statis calculated using the Log-rank (Mantel-Cox) test. (n = 6 mice for control, HSPC-Lipo and Ara-C group, C@Lipo group, and n = 11 mice for Ara-C@HSPC-Lipo group). c Representative flow cytometry plots positive cells) in bone marrow. Leukemic mice were euthanized on the day 21 to collect bone marrow cytometry analysis. d Quantitative analysis of leukemia cells in bone marrow. Data were presented a mice). e Representative flow cytometry plots of leukemia stem cells (CD34 + CD16/32 +) in bone ma treatments. f Quantitative analysis of leukemia stem cells in BM. Data were presented as mean ± s.d Representative flow cytometry plots of leukemic cells (GFP positive cells) in spleen. h Quantitative an in spleen. Data were presented as mean ± s.d. (n = 5 mice). i Quantitative analysis of leukemic cells peripheral blood. Data were presented as mean ± s.d. (n = 5 mice). j Representative spleen images different treatment. k Weight of Spleen. n = 5 mice. The data were presented as mean ± s.d. Statisti values was calculated via a two-tailed, unpaired Student’s t test and were indicated as * P

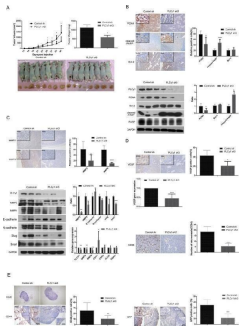

Depletion of PLCgamma1 suppresses growth and metastasis of gastric adenocarcinoma in a nude mou model. (A) Volume and weight of tumor samples from nude mice. (B) The protein levels of PCNA, cle Bcl-2 in the tumor samples were detected by Immunohistochemistry (Magnificationx100, x400) and W as described in Materials and Methods. (C) The levels of MMP2 and MMP9 in the tumor samples were Immunohistochemistry analysis as described in Materials and Methods (Magnificationx100, x400). The levels of MMP2, MMP9, E-cadherin(CDH1), N-cadherin(CDH2), snail(SNAIL), and slug(SLUG) in the tumo detected by Western Blotting and Real-time PCR analyses as described in Materials and Methods. (D) VEGF and CD34 and the mRNA level of VEGF in tumor samples were detected by Immunohistochemist analysis as described in Materials and Methods. The number of microvessels was accounted under OLY (Magnification x100, x400). (E) The lymphoid follicles in inguinal lymph nodes of nude mice were obs x41microscope, and the protein levels of CD44 and GFP in inguinal lymph nodes of nude mice was det Immunohistochemistry analysis as described in Materials and Methods (Magnificationx40, x400). Data ± S.D. of three independent experiments (* P < 0.05, ** P < 0.01, *** P < 0.001, **** P < 0.0001, vs re in PubMed under a CC BY license. PMID: 26811493

MSH2 knockdown increase the sensitivity of glioma cells to cisplatin. (A, B) The expression of stemnes including CD44 and SOX2 was detected in shCtrl and shMSH2 groups of U251 (A) and SHG-44 (B) cells sphere-forming abilities of U251 (C) and SHG-44 (D) cells were assessed by a 3D sphere formation ass MSH2 on cisplatin IC50 and cisplatin-induced cell apoptosis were evaluated in U251 (E) and SHG-44 (F as mean with standard deviation (SD) (n ≥ 3). p

BOSTER BIOLOGICAL TECHNOLOGY
3942 B Valley Ave, Pleasanton, CA 94566
888-466-3604 | support@bosterbio.com | www.bosterbio.com

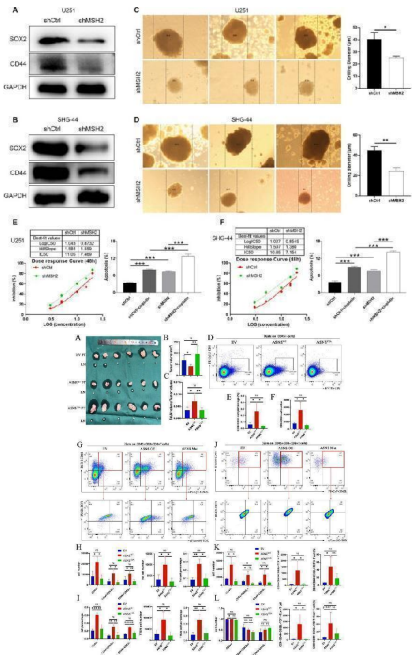

ASNS shapes the immune landscapes in metastatic TdLN and primary tumor site. Figure 5A-C. LN meta conducted on C57BL/6 mice with LLC-ASNS WT(n=6), ASNSC2A overexpression cells(n=6) and control tumor and popliteal lymph nodes were isolated at the end of the experiment, and primary tumor volur volume/tumor volume(C) was measured and analyzed. 5D-F. (D) Representative FACS profiles of CD8+ percentage(E) and number(F) of CD8+ subset in TIL cells isolated from primary tumor is shown. 5G-I. (profiles of the co-expression pattern of CD44 and CD62L, or the co-expression pattern of TCF-1and TO shown. The number(H) and percentage(I) of CD44+, CD44+CD62L+, CD44+CD62L-, Tsl and TTSM sub isolated from TdLN is shown. 5J-L. (J) Representative FACS profiles of the co-expression pattern of CD4 expression pattern of TCF-1and TOX in CD8+ T cells are shown. The number(K) and percentage(L) of C CD44+CD62L-, Tsl and TTSM subset in CD8+T cells isolated from primary tumor is shown.Index in Pub license. PMID: 41208878

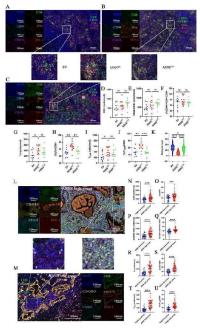

ASNS-high-expression metastases generated lymphocyte niches enriched with activated T cells, memo Figure 6A-C. Representative immunofluorescence staining images of metastatic TdLNs from LN metast number of CD8+ T cells in the metastasis locations within TdLNs (ASNSWT, n=6, ASNSC2A, n=5, and E number(E) and percentage(F) of CD44+CD8+T cells among all CD8 T cells in the metastasis locations n=6, ASNSC2A, n=5, and EV, n=4). 6G-H. The number(G) and percentage(H) of Tsl cells among all CD metastasis locations within TdLNs (ASNSWT, n=6, ASNSC2A, n=5, and EV, n=4). 6I-J. The number(I) ar cells among all CD8 T cells in the metastasis locations within TdLNs (ASNSWT, n=5, ASNSC2A, n=4, ar Quantitative estimates of the distance from ova+ to CD8+CD44+CD62L+TCF+(TTSM) (ASNSWT, n=6, n=4). 6L-M. Representative immunofluorescence staining images of metastatic TdLNs from NSCLC pat number(C) and percentage(D) of CD8+ T cells in the metastasis locations within TdLNs(ASNS high grou group, n=6). 6P-Q. The number (E) and percentage(F) of CD45RO+CD8+ T cells in CD8+T cells in the within TdLNs(ASNS high group, n=7, and ASNS low group, n=6). 6R-S. The number (G) and percentage cells in the metastasis locations within TdLNs(ASNS high group, n=7, and ASNS low group, n=6). 6T-U. percentage(J) of TTSM cells in CD8+T cells in the metastasis locations within TdLNs(ASNS high group, group, n=6).Index in PubMed under a CC BY license. PMID: 41208878

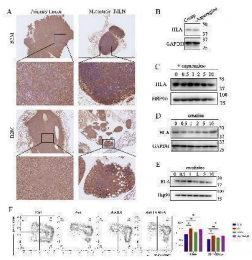

Representative IHC images showing the expression of B2M in primary tumor and LN metastasis from i implantation mouse model performed on C57BL/6 mice (upper, n=3) and popliteal lymph node implan performed on C57BL/6 mice (below, n=4). 3B. A549 cells were treated with low asparagine medium fo HLA was determined by western blotting. 3C-E. A549 cells were treated with asparagine (C), creatine (48 h. The expression of HLA was determined by western blotting. 3F. Representative FACS profiles are cells were treated with Asn, AABA or both for 48 h, and of the expression level of CD44 and CD62L was in PubMed under a CC BY license. PMID: 41208878

IHC analysis of CD44 using anti-CD44 antibody (A00052). CD44 was detected in paraffin-embedded se cancer tissue. Heat mediated antigen retrieval was performed in citrate buffer (pH6, epitope retrieval The tissue section was blocked with 10% goat serum. The tissue section was then incubated with 1ug/ Antibody (A00052) overnight at 4°C. Biotinylated goat anti-rabbit IgG was used as secondary antibody minutes at 37°C. The tissue section was developed using Strepavidin-Biotin-Complex (SABC)(Catalog # the chromogen.

BOSTER BIOLOGICAL TECHNOLOGY
3942 B Valley Ave, Pleasanton, CA 94566
888-466-3604 | support@bosterbio.com | www.bosterbio.com

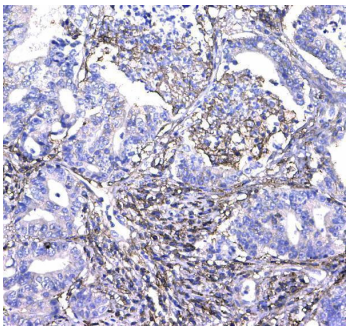

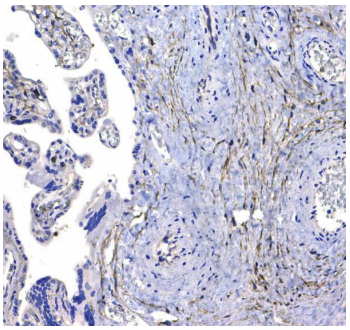

IHC analysis of CD44 using anti-CD44 antibody (A00052). CD44 was detected in paraffin-embedded se
tissue . Heat mediated antigen retrieval was performed in citrate buffer (pH6, epitope retrieval solutio
tissue section was blocked with 10% goat serum. The tissue section was then incubated with 1ug/ml ra
(A00052) overnight at 4°C. Biotinylated goat anti-rabbit IgG was used as secondary antibody and incu
37°C. The tissue section was developed using Strepavidin-Biotin-Complex (SABC)(Catalog # SA1022) w
chromogen.

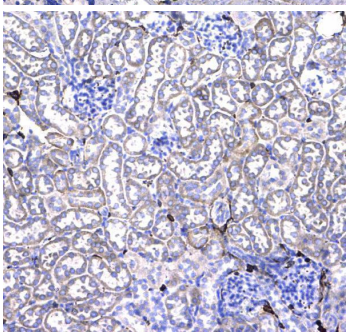

IHC analysis of CD44 using anti-CD44 antibody (A00052). CD44 was detected in paraffin-embedded se
tissue . Heat mediated antigen retrieval was performed in citrate buffer (pH6, epitope retrieval solutio
tissue section was blocked with 10% goat serum. The tissue section was then incubated with 1ug/ml ra
(A00052) overnight at 4°C. Biotinylated goat anti-rabbit IgG was used as secondary antibody and incu
37°C. The tissue section was developed using Strepavidin-Biotin-Complex (SABC)(Catalog # SA1022) w
chromogen.

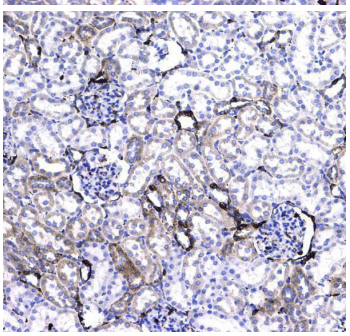

IHC analysis of CD44 using anti-CD44 antibody (A00052). CD44 was detected in paraffin-embedded se
. Heat mediated antigen retrieval was performed in citrate buffer (pH6, epitope retrieval solution) for 2
section was blocked with 10% goat serum. The tissue section was then incubated with 1ug/ml rabbit a
(A00052) overnight at 4°C. Biotinylated goat anti-rabbit IgG was used as secondary antibody and incu
37°C. The tissue section was developed using Strepavidin-Biotin-Complex (SABC)(Catalog # SA1022) w
chromogen.

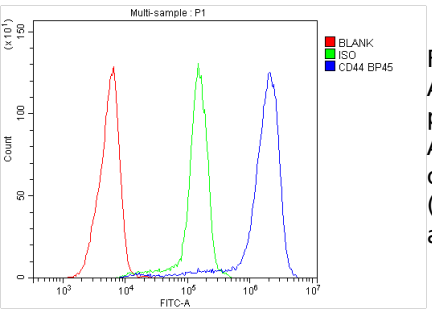

Flow Cytometry analysis of Jurkat cells using anti-CD44 antibody (A00052). Overlay histogram showing
A00052 (Blue line). To facilitate intracellular staining, cells were fixed with 4% paraformaldehyde and
permeabilization buffer. The cells were blocked with 10% normal goat serum. And then incubated with
Antibody (A00052,1ug/1x106 cells) for 30 min at 20°C. DyLight®488 conjugated goat anti-rabbit IgG (
cells) was used as secondary antibody for 30 minutes at 20°C. Isotype control antibody (Green line) wa
(1ug/1x106) used under the same conditions. Unlabelled sample without incubation with primary antib
antibody (Red line) was used as a blank control.

IF analysis of CD44 using anti-CD44 antibody (A00052) CD44 was detected in paraffin-embedded secti
tissues. Heat mediated antigen retrieval was performed in citrate buffer (pH6, epitope retrieval solutio
tissue section was blocked with 10% goat serum. The tissue section was then incubated with 1ug/mL r
Antibody (A00052) overnight at 4°C. DyLight®488 Conjugated Goat Anti-Rabbit IgG (BA1127) was use
at 1:100 dilution and incubated for 30 minutes at 37°C. The section was counterstained with DAPI. Visu

BOSTER BIOLOGICAL TECHNOLOGY
3942 B Valley Ave, Pleasanton, CA 94566
888-466-3604 | support@bosterbio.com | www.bosterbio.com

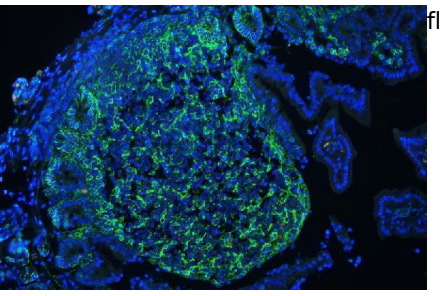

fluorescence microscope and filter sets appropriate for the label used.

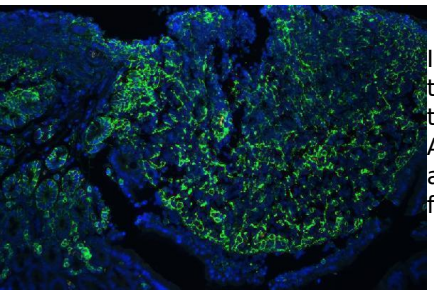

IF analysis of CD44 using anti-CD44 antibody (A00052) CD44 was detected in paraffin-embedded secti
tissues. Heat mediated antigen retrieval was performed in citrate buffer (pH6, epitope retrieval solutio
tissue section was blocked with 10% goat serum. The tissue section was then incubated with 1ug/mL r
Antibody (A00052) overnight at 4°C. DyLight®488 Conjugated Goat Anti-Rabbit IgG (BA1127) was use
at 1:100 dilution and incubated for 30 minutes at 37°C. The section was counterstained with DAPI. Visu
fluorescence microscope and filter sets appropriate for the label used.

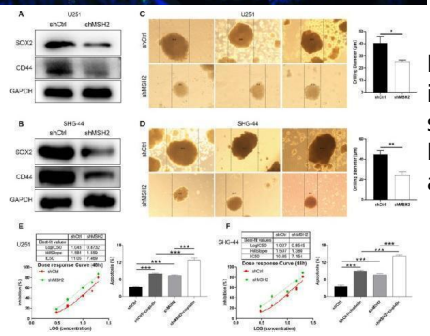

MSH2 knockdown increase the sensitivity of glioma cells to cisplatin. (A, B) The expression of stemnes
including CD44 and SOX2 was detected in shCtrl and shMSH2 groups of U251 (A) and SHG-44 (B) cells
sphere-forming abilities of U251 (C) and SHG-44 (D) cells were assessed by a 3D sphere formation ass
MSH2 on cisplatin IC50 and cisplatin-induced cell apoptosis were evaluated in U251 (E) and SHG-44 (F
as mean with standard deviation (SD) (n ≥ 3). p

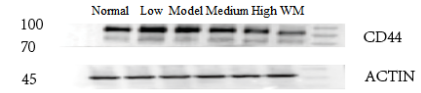

Western blot analysis of CD44 using anti-CD44 antibody (A00052). Electrophoresis was performed on a
70V (Stacking gel) / 90V (Resolving gel) for 2-3 hours. The sample well of each lane was loaded with 3
reducing conditions. Lane 1: Normal group-rat colon tissue lysates, Lane 2: Triditional Chinese medicin
dose)-rat colon tissue lysates, Lane 3: Model group-rat colon tissue lysates, Lane 4: Triditional Chinese
(medium dose)-rat colon tissue lysates, Lane 5: Triditional Chinese medicine treatment(high dose)-rat
Lane 6: Western medicine treatment-rat colon tissue lysates. After electrophoresis, proteins were tran
nitrocellulose membrane at 150 mA for 50-90 minutes. Blocked the membrane with 5% non-fat milk/TB
The membrane was incubated with rabbit anti-CD44 antigen affinity purified polyclonal antibody (Cata
overnight at 4°C, then washed with TBS-0.1%Tween 3 times with 5 minutes each and probed with a go
secondary antibody for 1 hour at RT. The signal is developed using an Enhanced Chemiluminescent de
(Catalog # EK1002) with ChemiDoc MP system. A specific band was detected for CD44 at approximate
band size for CD44 is at 82 kDa.

49 Publications Citing This Product

1. PubMed ID: PMID:25120772, Effects of BMSCs interactions with adventitial fibroblasts in transdifferentiation and u

2. PubMed ID: 10.3390/molecules21091246, Comparison of the Antioxidant Effects of Quercitrin and Isoquercitrin: U
6?-OH Group

3. PubMed ID: 10.3390/molecules22071165, Role of the p-Coumaroyl Moiety in the Antioxidant and Cytoprotective E
Glycosides: Comparison of Astragalin and Tiliroside

Visit bosterbio.com/anti-cd44-picoband-trade-antibody-a00052-boster.html to see all 49 publications.

BOSTER BIOLOGICAL TECHNOLOGY
3942 B Valley Ave, Pleasanton, CA 94566
888-466-3604 | support@bosterbio.com | www.bosterbio.com

Anti-CD44 Antibody

For Research Use Only. Not for use in diagnostic procedures.